CrystEngComm

Accepted Manuscript

ROYAL SOCIETY OF CHEMISTRY

www.rsc.org/crystengcomm

Quasi-Enantiomeric Single-Nucleoside and *Quasi*-Racemic Two-Nucleosides Hydrochloride Salts and Ruthenium Complexes of Cytidine and 2',3'-Dideoxycytidine Analogs Unveiling the Negligible Structure-Driving Role of the 2',3'-Moieties

Felipe Terra Martins,[a,] Rodrigo S. Corrêa,[b] Alzir Azevedo Batista,[b] Javier Ellena[c]*

[a]Instituto de Química, Universidade Federal de Goiás, Campus Samambaia, CP 131, 74001-970, Goiânia, GO, Brazil; [b]Departamento de Química, Universidade Federal de São Carlos – UFSCar, Rodovia Washington Luís KM 235, CP 676, 13561-901, São Carlos, SP, Brazil; [c]Departamento de Física e Informática, Instituto de Física de São Carlos, Universidade de São Paulo, CP 369, 13560-970, São Carlos, SP, Brazil

* To whom correspondence should be addressed. E-mail: felipe@ufg.br

Phone: +55 62 3521 1097. Fax: +55 62 3521 1167

Abstract: Insights into the structural basis of nucleosides molecular organization have been gotten from crystal engineering researches. Here we have investigated the role of differences at the 3'-position of the five-membered ring in the determination of molecular conformation and crystal packing of *quasi*-enantiomeric cytidine-based nucleosides. Firstly, a hydrochloride salt of zalcitabine (2',3'-dideoxycytidine) isostructural to lamivudine (2',3'-dideoxy-3'-thiacytidine) hydrochloride was prepared. The $R_2^1(6)$ motif responsible for pairing between nucleosides and counterion as well as the assembly of chains and sheets with 2_1-screw axis symmetry related ionic pairs were observed in both salts even with lamivudine differing from zalcitabine for opposite chirality of C1' and C4' carbons and for a sulfur atom at 3'-position rather than a methylene group. Based on the isostructurality between zalcitabine hydrochloride and lamivudine hydrochloride, but with crystal structures which are *quasi*-enantiomeric, a hydrochloride salt having both nucleosides into a single crystal form was designed in this study. The obtained hybrid structure is a *quasi*-racemate in which chains assembled with $R_2^1(6)$-paired lamivudine and chloride can be related by pseudo inversion symmetry to that made up of zalcitabine and chloride but with antiparallel growth direction. In addition, the first examples of ruthenium(II) coordination complexes with cytidine nucleosides are reported here. The *trans*-*bis*-(triphenylphosphine)(lamivudinate)(2,2'-bipyridine)ruthenium(II) perchlorate and *trans*-*bis*-(triphenylphosphine)(cytidinate)(2,2'-bipyridine)ruthenium(II) perchlorate complexes have presented the same coordination geometry but with opposite chirality and similar chains assembled with translation symmetry related complexes intercalated by water despite of a greater molecular difference such as 2'-CH_2 and 3'-S moieties in lamivudine rather than CH_2OH ones in both positions of cytidine.

1. Introduction

The comprehension of structural phenomenon driving molecular assembly in crystals has been extensively investigated nowadays.[1] Supramolecular functionality and synthon concepts have provided an advance in understanding why certain packing frameworks are frequently found in crystals while others do not.[2] Besides becoming easier the interpretation of complex crystal architectures by mean of recognition of most frequent intermolecular interactions patterns, these concepts allow one to predict how molecules will be assembled into supramolecular motifs.[3] Sometimes, even crystal system and space groups can be predicted successfully on the basis of recognition of robust synthons and persistence of supramolecular motifs.[4] Once the role of synthons and crystal packing entities in the structures assembly could be understood in the practice, crystal engineers can explore them to design new polymorphs and multicomponent molecular crystals with desired solid state properties. In fact, crystal engineering strategy based on such knowledge is one of the most important routes to modulate and fine tune macroscopic features of a functional material in the solid state.[5] Concerning pharmaceuticals, several performance improvements such as increasing in solubility, dissolution rate, stability and flow property among others have been achieved with crystal forms rationally conceived invoking synthons and intermolecular isostructurality.[6] In this sense, multicomponent molecular crystals of active pharmaceutical ingredients (APIs) are widely investigated due to welcome possibility to manipulate a functional and/or technical feature in association with practical preparation procedures chemically designed without serendipity, higher yield, reproducibility, and purity.[7]

Lamivudine (β-L-2',3'-dideoxy-3'-thiacytidine, 3TC) is an API of the nucleoside reverse transcriptase inhibitors (NRTI) class used against both AIDS (HIV) and hepatitis B (HBV) viruses. It was originally marketed by GlaxoSmithKline pharmaceutical company under the brand name EPIVIR®. This drug is a remarkable example in which crystal engineering can be successfully employed to improve its solid

state properties related to pharmaceutical performance.[8] Solubility has been increased with salts thereof.[8] Besides that, lamivudine is a small molecule template to give insight into the understanding of multicomponent molecular crystal formation in NRTIs as well as in nucleic acid double-stranded helix assembly,[9] becoming it an attractive API for crystal engineering researches.

For instance, synthon conservation and isostructurality has been demonstrated to occur in lamivudine salts with saccharin and maleic acid even though their great molecular differences, revealing the robustness of a $R_2^2(8)$ [10] hydrogen-bonded cycle responsible for the pairing between drug and counterions and the persistence of supramolecular motifs as chains and sheets made up of 2_1-screw axis symmetry related ionic pairs.[4] On the other hand, such a synthon was not observed in hydrogen phthalate salts anhydrate and hemihydrate of lamivudine having a counterion with the same synthon ability of the other two salts.[5]

Lamivudine molecule presents two chiral carbons, C1' and C4', with *S* and *R* absolute configurations. It is known that its anhydrous form II is isostructural to zalcitabine (2',3'-dideoxycytidine).[11] The last is also a NRTI API marketed under the brand name HIVID® by Roche industry, but it is few indicated for anti-HIV therapy nowadays. It differs from lamivudine for the opposite chirality of its C1' and C4' carbons (*R* and *S*, respectively), and for the 3'-CH_2 in the five members ring instead of the 3'-sulphur in the counterpart. Both cytidine-like nucleosides exhibit the same packing and conformation into tetragonal unit cells containing enantiomorphic symmetry elements, namely, $P4_32_12$ (lamivudine) and $P4_12_12$ (zalcitabine). Therefore, isostructurality of lamivudine and zalcitabine provides a clue on their ability to form *quasi*-enantiomeric crystals even if their 3'-position moiety is not the same.

Here we study if the ability of lamivudine and zalcitabine to form *quasi*-enantiomeric crystals could be extended to multicomponent crystal forms containing them. For this purpose, and based on the

known synthetic route of lamivudine hydrochloride (**1**)[12], a hydrochloride salt of zalcitabine was prepared. Zalcitabine hydrochloride (**2**) is isostructural to **1**. Based on that, we proceed to co-crystallization of both APIs. Interestingly, lamivudine zalcitabine hydrochloride (**3**) crystallized as a *quasi*-racemate, with both APIs related by a pseudo inversion center. These results show the meaningless role of differences at the 3'-position in the determination of molecular conformation and crystal packing (see Scheme 1 for chemical structures). Furthermore, in this study we prepared the first example of ruthenium(II) complexes with cytidine-like ligands, namely, *trans*-[$Ru(PPh_3)_2$(3TC)(bipy)]ClO_4 (**4**) and *trans*-[$Ru(PPh_3)_2$(CYD) (bipy)]ClO_4 (**5**), where PPh_3 means tryphenylphosphine, bipy refers to 2,2'-bipyridine, and the ligands 3TC and CYD are lamivudinate and cytidinate, respectively. Ruthenium complexes with nucleosides are known only with adenosine monophosphate and guanosine,[13] while cytidine and analogs are shown only to form coordination complexes with osmium.[14] Despite the differences determined by the presence of CH_2OH moieties at 2' and 3' positions of cytidine rather than CH_2 and S in lamivudine, both complexes show the same coordination geometry. Moreover, they present assemblies of supramolecular chains made up of translation symmetry related complexes intercalated by water units.

Insert Scheme 1

2. Material and Methods

*2.1 Preparation of **2** and **3***

Anhydrate forms of lamivudine and zalcitabine were used for preparation of **2** and **3**. Lamivudine was acquired from Instituto Nacional de Controle de Qualidade, FIOCRUZ (lamivudine purity of 99.55 ± 0.07 mol % and melting temperature of 175.6 ± 0.3 °C, both determined by differential scanning calorimetry according to the ASTM E928 standard specification). Zalcitabine was purchased from Sigma-Aldrich® (HPLC grade). Some crystals of both APIs were directly isolated from their sample batch and were first analyzed by single crystal X-ray diffraction technique prior using them in the preparation of **2** and **3**. Indexed unit cell constants have matched to those reported in the literature for their anhydrated crystal structures, which confirmed the authenticity of the samples.

The preparation of **2** follows the procedure described previously for synthesis of **1**,[12] but changing the API. Zalcitabine (10 mg, 0.04 mmol) was dissolved in isopropyl alcohol (5 ml, 66 mmol) on a water bath (308 K) under stirring (5 min). Next, a 0.28 mol L^{-1} solution of hydrochloric acid in water (0.25 ml, 0.07 mmol) was added under stirring (5 min, 298 K) to the room temperature cooled solution of zalcitabine in isopropyl alcohol. Plate-shaped crystals of **2** were grown on the bottom of glass crystallizers after slow evaporation of the acid solution upon standing (7 days, 298 K). The same protocol was used for preparation of **3**, expect for simultaneous dissolution of both lamivudine (5 mg, 0.022 mmol) and zalcitabine (5 mg, 0.023 mmol) in isopropyl alcohol (5 ml, 66 mmol), following the next procedures above described.

*2.2 Synthesis of **4** and **5***

The **4** and **5** complexes were synthesized using same procedure using the *cis*-$[RuCl_2(PPh_3)_2(bipy)]$ as starting complex that was prepared according to the literature.[15] The ligand lamivudine (0.12 mmol, 28.0 mg) or cytidine (0.12 mmol, 30.0 mg) was dissolved in 50 mL of a

mixture of dichloromethane/methanol (1:1 *v/v*) with 20 μL of triethylamine and $NaClO_4$ (0.12 mmol; 15.0 mg). After, 100 mg (0.11 mmol) of the *cis*-$[RuCl_2(PPh_3)_2(bipy)]$ precursor was added and each reaction was kept under reflux and stirred for 24 h, under argon atmosphere. The final orange solutions were concentrated to *ca.* 2 mL and 10 mL of water was added in order to obtain orange precipitate. The solids were filtered off and washed with warm water and diethyl ether and dried under *vacuum*. Single crystals of **4** were grown by slow evaporation of an acetone/water (9:1 *v/v*) at room temperature, whereas crystals of **5** were grown by diethyl ether diffusion into a dichloromethane solution of the complex.

(4): yield of 110 mg (85%). Anal. Calc. for $RuC_{54}H_{48}N_5O_3P_2S.ClO_4.H_2O$: exp. (calc) C, 57.38 (57.52); H, 4.40 (4.47); N, 6.15 (6.21); S, 2.76 (2.84) %. Molar conductance (μS/cm, CH_2Cl_2) 28.2. $^{31}P\{^1H\}$ NMR (162 MHz, $CDCl_3$, 298 K): δ(ppm) 36.8 (s); ^1H NMR (400 MHz, $CDCl_3$, 298 K):δ(ppm) 10.50 (1H, C7-H of bipy) and 9.30 (1H, C16-H of bipy); 7.50-6.90 (30H aromatic hydrogen atoms of PPh_3 and 6H aromatic hydrogen atoms of bipy); 6.47 (1H, C6-H of 3TC); 6.01 (1H, C1'-H of 3TC); 5.28 (1H, C4'-H of 3TC); 4.48 (1H, C5-H of 3TC); 3.93 and 3.81 (2H, C5'-H of 3TC); 3.19 and 2.81 (2H, C2'-H of 3TC). ^{13}C NMR (400 MHz, $CDCl_3$, 298 K): δ(ppm) 169.6 (C4); 158-156 (C2 and 4C of bipy); 135-121 (6C of bipy, 36C of PPh_3 and C6 of 3TC); 96.4 (C5); 87.9 (C1'); 83.9 (C4'); 64.6 (C5'); 35.9 (C5'). UV-Vis (CH_2Cl_2, 10^{-5} M): λ/nm (ε/$mol^{-1}Lcm^{-1}$) 338 (8.920 x 10^3), 436 (3.768 x 10^3).

(5): yield of 100 mg (77%). Anal. Calc. for $RuC_{55}H_{50}N_5O_5P_2S.ClO_4.2H_2O.CH_3OH$: exp. (calc) C, 56.62(56.45); H, 5.03(4.91); N, 5.84(5.88) %. Molar conductance (μS/cm, CH_2Cl_2) 22.7. $^{31}P\{^1H\}$ NMR (162 MHz, $CDCl_3$, 298 K): δ(ppm) 37.7 (s); ^1H NMR (400 MHz, $CDCl_3$, 298 K):δ(ppm) 10.46 (1H, C7-H of bipy) and 9.23 (1H, C16-H of bipy); 7.50-6.90 (30H aromatic hydrogen atoms of PPh_3 and 6H aromatic hydrogen atoms of bipy); 6.49 (1H, C6-H of CYD); 5.78 (1H, C1'-H of CYD); 5.33 (1H, C4'-

H of CYD); 4.98 (1H, C5-H of CYD); 3.35 and 3.23 (1H, C3'-H and C2'-H of CYD); 3.90 and 2.82 (2H, C5'-H of CYD). ^{13}C NMR (400 MHz, $CDCl_3$, 298 K): δ(ppm) 169.6 (C4); 158-156 (C2 and 4C of bipy); 136-121 (6C of bipy, 36C of PPh_3 and C6 of CYD); 95.4 (C5); 86.0 (C1'); 75.4 (C4'); 71.4 (C3'); 65.9 (C2'); 62.4 (C5'). UV-Vis (CH_2Cl_2, 10^{-5} M): λ/nm (ε/mol^{-1}Lcm^{-1}) 340 (7.244 x 10^3), 440 (3.998 x 10^3).

2.3 Structure determination

Well-grown single crystals of **2** - **5** were selected after full solvent matrix evaporation. They were mounted on a κ-goniostat and exposed at room temperature to graphite-monochromated X-ray beam (Mo Kα, $\lambda = 0.71073$ Å) using an Enraf-Nonius Kappa-CCD diffractometer equipped with a CCD camera of 95 mm. In the case of **2** and **3**, low-temperature data collection was also performed using a cold N_2 gas blower cryogenic device (Oxford Cryosystem, Oxford), revealing the inexistence of crystal-to-crystal phase transformation between the evaluated temperature range based on the fact that there are not straight differences in the unit cell constants (see Table S1) and the solved structures do not differ under room and low temperatures of X-ray diffraction data collect.

Room temperature X-ray diffraction data of **3** had low intensity even at medium resolution. Consequently, dataset of nonsatisfactory overall quality was gotten. But, fortunately, this was not observed for dataset collected at low temperature. Refinements on low temperature data were stable and converged more easily, resulting in acceptable *R*-factors for crystal structure of **3**. Furthermore, a positional disorder in the whole hydroxymethylene branch of lamivudine of **3** can be reliably modeled based on low temperature dataset. This disorder was refined over two occupancy sites for each atom of the 5'-CH_2OH moiety, with constrained site occupancy (s. o.) factors of 60% (the atom fractions

labeled as C5'L, H5'xL, H5'yL, O5'L and H5'OL) and 40% (the atom fractions labeled as C5'L', H5'xL', H5'yL', O5'L' and H5'OL').

The crystallographic softwares were used as follows: COLLECT[16] (X-ray diffraction collect strategy with φ scans and ω scans and with κ offsets, besides frame acquision monitoring), HKL Denzo-Scalepack[17] package of softwares (indexing, integration and scaling of raw data), SHELXS-97[18] (structure solving), SHELXL-97[18] (structure refinement), MERCURY[19] and ORTEP-3[20] (structure analysis and graphical representations). The structures were solved using the direct methods of phase retrieval. All non-hydrogen atoms of asymmetric unit were promptly assigned from the electronic density Fourier synthesis, being then their positional and thermal parameters refined by full-matrix least squares method based on F^2. Free anisotropic and fixed isotropic atomic displacement parameters were set for non-hydrogen and hydrogen atoms, respectively. The isotropic thermal displacement parameters of the C—H and N—H hydrogen atoms were 20% greater than the equivalent isotropic parameter of the corresponding atom. For the O—H hydrogen atoms, this percentage was set to 50%. Concerning the positions of hydrogens, C—H bond distances were stereochemically defined according to riding model. Therefore, their positional parameters were constrained in the refinements. The coordinates of O—H, N—H and N^+—H hydrogen atoms were primarily defined as those of the electronic density peaks located from the difference Fourier map and refined freely in **2,** contrarily to 3-5 in which their coordinates were fixed following the riding model after the residual electronic density peak corresponding to hydrogens in query have been properly identified from difference Fourier map.

3. Results and Discussion

We have previously obtained **1** from a solvent matrix made up of 0.28 mol L^{-1} solution of hydrochloric acid in water (0.25 mL) and isopropyl alcohol (5 mL).[12] Based on the isostructurality of anhydrous forms of lamivudine and zalcitabine[11] crystallizing in enantiomorphic tetragonal space groups $P4_32_12$ and $P4_12_12$, respectively, we were interested to know if both API could crystallize together in a multicomponent salt. In fact, lamivudine and zalcitabine are 2',3'-dideoxycytidine analogs differing in a sulfur atom at 3'-position in the first rather than a methylene group in the last and for the chirality of their asymmetry centers. The two chiral carbons, C1' and C4', show *S* and *R* absolute configurations in lamivudine and *R* and *S* ones in zalcitabine, respectively. Based on the fact that their anhydrate phases have *quasi*-enantiomeric structures,[11] one can realize that the isosteric replacement of methylene in zalcitabine with sulfur atom in lamivudine at 3'-position have not a structure-driving role in their molecular conformation and intermolecular assembly. Therefore, **2** was expected to crystallize isostructurally to **1**, which has been successfully realized.

The salt **2** was obtained using the same solvent matrix employed to prepare **1**. The pH value was below two for the crystallization medium of both APIs due to the hydrochloric acid concentration in the solvent system. Considering the pK_a values of zalcitabine (4.34)[21] and lamivudine (4.30)[22], protonated forms of both drugs were at least 200-fold more than neutral ones in the bulk of acid crystallization batches, even before beginning the solvent evaporation. In this way, the crystallization of phases only made up of positively charged drug molecules and chloride counterions was possible. It is important to comment that the hydrochloride salts have been obtained as isostructural solid state phases of opposite chirality due to the use of achiral solvents such as water and isopropyl alcohol in both cases.

Both hydrochloride salts crystallize in the $P2_1$ space group with one cation, $(drug)^+$, and one chloride anion in the asymmetric units (Fig. 1 and Table S1). The drug conformations are almost identical in **1** and **2**, with the cytosine and oxathiolane rings adopting *anti* and C3'-*endo* puckering conformations, respectively (see Table S2 for torsions on the N1—C1' bridge and into the five-membered ring describing these conformations). The hydroxyl group conformation is also the same in both salts assuming an equatorial position on the same side of the CH_2 or sulfur at 3'-position of the five-membered ring (see Table S2 for torsions around the 5'-CH_2OH branch describing this conformation). The dihedral angles of **2** are similar to the corresponding ones of **1**, but with opposite signals. This reflects the conformational similarity between them but with opposite chirality.

Insert Figure 1

The crystal packing features of **1** and **2** were also conserved. Both structures were assembled with ionic pairs made up of drug cation and chloride counterion held together through two hydrogen bonds in which protonated cytosine ring of the drugs is a donor through its imine and amine moieties to a same in-plane chloride anion (see Table S2 for planarity descriptors). This gives rise to a pairing with bifurcated hydrogen bonding motif. The other NH_2 hydrogen that is not involved in the pairing with chloride anion in the bifurcated hydrogen bonds is also interacting with a 2_1-screw axis symmetry related chloride anion, which is out of the cytosine plane. Such hydrogen bonding pattern is responsible for the assembly of one-dimensional chains parallel to the [010] direction made up of alternate drug cations and chloride anions. Along this direction, API units related by 2_1-screw axis symmetry are connected through a O—H•••O hydrogen bond between the 5'-hydroxyl and 2-carbonyl groups. This contact acts as a cross-linker between the [010]-packed chains along the [10-1] direction, giving rise to

2D sheets (Fig. 2). The 3D crystal packing of both hydrochloride salts is completed by face-to-tail π-π base-stacking interactions along the [100] direction (Fig. 2), with intersheet spaces measuring 3.22(4) Å and 3.30(1) Å in **2** and **1**, respectively (see Fig. S1 for complete geometry of the stacking interaction). Furthermore, chloride channels are assembled parallel to the stacking direction. There is not non-classical hydrogen bonds involving 3'-CH_2 moiety of zalcitabine in its hydrochloride salt, as well as sulfur atom does not participate of significant intermolecular contacts in **1**. The shortest separation between the 3'-CH_2 carbon and a hydrogen bonding acceptor atom is 4.110(3) Å [C3'•••O5'^{i} (i) = - 1 + x; y; z)], ruling out the possibility of occurrence of any weak hydrogen bonding between them. This reinforces the fact that the moiety at 3'-position of the 5 member ring does not drive the crystal structure of the cytidine analogs. The geometrical parameters of the intermolecular interactions present in **2** are listed in Table S3.

Insert Figure 2

Based on the isostructurality and chirality in the zalcitabine hydrochloride and lamivudine hydrochloride, we decide to explore the crystallization of a two-drug system in the form of a hydrochloride salt since it could lead to either a physical mixture or *quasi*-racemate. *Quasi* refers to the 3'-position moiety differing for lamivudine and zalcitabine. After a few attempts it was possible to obtain crystallized this multicomponent system from the same solvent matrix used in the crystallization of the zalcitabine and lamivudine hydrochloride, using a 1:1 lamivudine:zalcitabine stoichiometry. The two-drug salt **3** crystalize in the triclinic space group *P*1 (Table S1), showing a pseudo inversion center.

One protonated molecule of lamivudine, another one of zalcitabine, and two chloride counterions compose the asymmetry unit (Fig. 3).

The same hydrogen bonding pattern between cytosine and chloride counterion into chains found in the two isostructural salts of only one API also occurs in the salt of both APIs (Fig. 4). However, these chains are made up of either lamivudine or zalcitabine in **3** rather than alternating them into every chain. These chains therefore contain just one API. In addition, in **3** the out of the pairing NH_2 hydrogen atom is hydrogen bonded to a chloride counterion related by translation symmetry instead of the screw axis present in **1** and **2** (see Figs. 2 and 4 for comparison). In **3**, such chloride anion hydrogen bonded to out of the pairing NH_2 hydrogen is more coplanar to cytosine than in **1** and **2**. Furthermore, in **3** the paired chloride counterion accepting two hydrogen bonds from cytosine of zalcitabine is less coplanar with the heterocycle than the out of the pairing one, which accepts only one hydrogen bond, unlike what happens in **1, 2** and the chloride anion paired with lamivudine in **3** (see Table S2 for planarity descriptors).

Insert Figure 3

Even though lamivudine and zalcitabine are not alternated into the chains running along the [100] direction, chains assembled with either lamivudine or zalcitabine are running on opposite senses parallel to the [010] direction and are alternately packed through offset face-to-face π-π stacking interactions along the [010] direction, with stacking distances of 3.28(2) Å and 3.35(6) Å (Fig. 4 and Fig. S1 for complete geometry of the stacking interaction). The largest stacking distance occurs between neighboring chains which are further stabilized through strong hydrogen bonds between the hydroxyl group of either lamivudine (that with s. o. factors of 40%) or zalcitabine and the chloride counterion paired with one another stacked drug. This gives rise to a side closed framework of two

pseudo centrosymmetric chains, namely, $[(\text{lamivudine})^{+}\text{Cl}^{-}]_n$ and $[(\text{zalcitabine})^{+}\text{Cl}^{-}]_n$ (Fig. 4). The geometry of all hydrogen bonds present in **3** is shown in Table S3.

Is important to note that the hydrogen bond donation from the hydroxyl group of molecules belonging to a given chain to a chloride counterion of another one on its top, as observed in **3,** is only possible due to opposite chirality of asymmetry centers of the lamivudine and zalcitabine molecules. This allows to orient both five-membered rings toward the same interchain space, and, consequently, to form the O5'—H•••Cl hydrogen bonds in both sides of the face-to-face stacked chains. On the other hand, a face-to-tail stacking is required when only one API is present, as it happens in **1** and **2**. With this stacking mode, such hydrogen bond is sterically hindered to assemble on the two sides of stacked chains. This stacking mode was observed in these structures, although no hydrogen bond between hydroxyl moiety and chloride counterion takes place there.

Insert Figure 4

In addition, the other hydroxyl group fraction of lamivudine with s.o. factors of 60 % is a hydrogen bonding donor to the hydroxyl oxygen of zalcitabine. This O5'L—H•••O5'Z hydrogen bond together with the π-π interaction having the largest separation between stacked nucleobases are responsible for alternating lamivudine and zalcitabine along the [11-1] direction (Fig. 4).

As expected from our crystal engineering strategy based on the isostructurality of **1** and **2**, cytosine and oxathiolane conformations in **3** show an *anti* and a C3'-*endo* puckering conformation, respectively (see Fig. 3 and Table S2). In this structure, the hydroxyl group of lamivudine with major s. o. factors of

60% is in the equatorial position on the same side of sulfur, as well as in **1** (Table S2). On the other hand, in **3** the hydroxyl group of zalcitabine and that of lamivudine with minor s. o. factors of 40% differ from those observed in **1** and **2**. They are in the equatorial position on the opposite side of the 3'-position moiety (Table S2).

The ability of cytidine-based nucleosides to form *quasi*-enantiomeric crystals despite of molecular differences in the five-membered ring has been also assessed in ruthenium coordination complexes containing lamivudine and cytidine. We here prepared tansition metal coordination complexes of cytidine-based nucleosides, namely, *trans*-$[Ru(PPh_3)_2(3TC)(bipy)]ClO_4$ (**4**) and *trans*-$[Ru(PPh_3)_2(CYD)(bipy)]ClO_4$ (**5**), where PPh_3 means tryphenylphosphine, bipy refers to 2,2'-bipyridine, and the ligands 3TC and CYD are lamivudinate and cytidinate, respectively (Fig. 5).

Insert Figure 5

Their asymmetric unit shows one cationic Ru(II) coordination complex in **4** and two in **5.** The asymmetric unit of **4** also contains one water and one acetone molecule as well as one perchlorate counterion. The asymmetric unit of **5** also contains three water molecules and one methyl alcohol, all of them with 50% s. o. factors each, one diethyl ether and two perchlorate counterions (Figs. S2 and S3). The structure of **4** was solved in the orthorhombic space group $P2_12_12_1$, while **5** has crystallized in the monoclinic space group $P2_1$ (Table S1).

Analyzing the molecular geometry of the two complexes, a distorted octahedral geometry around the ruthenium(II) metal center is observed. The most important bond lengths and angles around the

coordination center of both complexes are shown in Table S4. All N–Ru–N bond angles on the equatorial position are far from the expected value of 90° in both complexes due to the tension of the four and five-membered chelate rings. On the other hand, in both cases the less tensioned P–Ru–N bond angles are closer to 90°. Both complexes present the same stereochemistry (Fig. 5), in which the phosphorus atoms of the PPh_3 ligand do adopt a *trans* configuration with P1–Ru–P2 bond angles close to 180°. Ellipsoid plots for **4** and **5** can be found in Supplementary Information (Figs. S2 and S3).

Interestingly, coordination geometry was identical in **4** and **5**, in which both lamivudine and cytidine ligands are coordinated to Ru(II) as a anionic bidentate N,N-donor through their imine N3 and deprotonated amine N4 nitrogen atoms. In both cases the N3 and N4 are *trans* to the nitrogen atoms of the bipy ligand (N2 and N5). As can be seen in Table S4, the N3–C4 and C4–N4 bond lengths are similar, suggesting that the N3–C4–N4 group form a negatively charged resonant moiety.

Cytosine adopts an intermediate conformation between *anti* and *syn* in **4** and **5**, while the five-membered ring puckers as C1'-*exo* in **4** and also in one of the two crystallographically independent complex units of **5**, namely, that labeled as cytidine A (see torsion angles in Table S5). Both cytosine and sugar conformations are unusual in canonical nucleosides, although they have been previously reported in the lamivudine hydrochloride hemihydrate.[9a] The conformation of the 5'-CH_2OH branch in **4** is also similar to that found in cytidine A unit of **5**. In both cases the OH oxygen atom at the C5' axial position points toward the same side of the 3'-position group (Fig. 5). Both complexes also show a hydrogen bond between O5' and a water molecule.

Besides the same coordination geometry, supramolecular building units are also conserved in **4** and **5** despite of the differences in their molecular backbones, namely, the presence of 2'-CH_2 and 3'-S moieties in lamivudine rather than CH_2OH ones in cytidine. The structure of **4** is mainly stabilized by

hydrogen bonds in which the water molecule is a double donor to both hydroxyl and carbonyl oxygens of the lamivudine ligand. This gives rise to infinite 1D chain along the [100] direction made up of alternate complex and water units (Fig. 6). Into the chain backbone, there are only translation-symmetry related complex and water species. In this structure, lamivudine is linked by a hydrogen bond to the perchlorate counterion through its deprotonated amine NH moiety (Fig. 6). Supramolecular interactions of **5** are similar to the ones found in **4** (Fig. 6). However, in **5**, each **4**-like chain is assembled with only either cytidine A, whose conformation is related to lamivudine in **4** (Fig. 5), or cytidine B. Indeed, cytidine B and lamivudine-like cytidine A differ because the cytosine and sugar moieties of cytidine B are present in the *anti* and C3'-*endo* conformations rather than in a conformation intermediate between *syn* and *anti* and C1'-*exo* like in cytidine A and lamivudine. The similarity between the cytidine ligands is in the 5'-OH axial position. This conformational similarity reflects the assembly of the one-dimensional chains as occurs in **4** (Fig. 6).

Insert Figure 6

In **5** the cytidine A units related by a translation symmetry are intercalated by one water molecule disordered over two sites showing 50% occupancy each. One water fraction is hydrogen bonded to one hydroxyl oxygen and the other one to the carbonyl oxygen. Meanwhile those of cytidine B are intercalated by a water molecule with just 50% of occupancy factor acting as dual donor to the neighboring nucleoside molecules (Fig. 6). Perchlorate is also a hydrogen bond acceptor from the deprotonated amine groups of both cytidine A and B units, like in **4**. However, the perchlorate counterion linked to the cytidine B unit accepts a hydrogen bond from the hydroxyl moiety at 3'-position of another cytidine B unit related by a 2_1-screw axis. This last contact helps to rationalize the C3'-*endo* puckering of cytidine B contrasting to C1'-*exo* of cytidine A and lamivudine (Fig. 5).

4. Conclusions

Isostructurality between single-drug hydrochloride salts of lamivudine and zalcitabine reveals their ability to assemble *quasi*-enantiomeric crystals even in multicomponent crystal forms. The 3'-position moiety does not influence molecular conformation and supramolecular architecture of the single-drug hydrochloride salts of lamivudine and zalcitabine, as also occurs in their anhydrate phases. Furthermore, these *quasi*-enantiomeric hydrochloride salts are able to form a *quasi*-racemate when crystallized together. The two-drug hydrochloride salt of lamivudine and zalcitabine has pseudo centrosymmetric chains assembled with either lamivudine or zalcitabine and chloride units. Based on this finding, we believe that the tendency of *quasi*-enantiomeric nucleosides to assemble *quasi*-racemate should be better explored when searching new multicomponent crystal forms thereof.

The first examples of transition metal coordination complexes containing cytidine analogs, *trans*-*bis*-(triphenylphosphine)(lamivudinate)(2,2'-bipyridine)ruthenium(II) perchlorate and *trans*-*bis*-(triphenylphosphine)(cytidinate)(2,2'-bipyridine)ruthenium(II) perchlorate complexes were reported in this study. They show the same coordination geometry and similar supramolecular building blocks despite of the presence of 2'-CH_2 and 3'-S moieties in lamivudine rather than CH_2OH ones in cytidine. Therefore, the effect of these 2',3'-positions groups in the crystal structure seems to be negligible as well as in the hydrochloride salts.

Acknowledgment. We thank the Brazilian Research Council CNPq (Conselho Nacional de Desenvolvimento Científico e Tecnológico) for the financial support (Processo 472623/2011-7 - Universal 14/2011). R.S.C. thanks FAPESP for a PhD fellowship (Grant number 2009/08131-1). We thank Altivo Pitaluga Jr. (Fundação Oswaldo Cruz - FIOCRUZ, Manguinhos, Rio de Janeiro, Brazil) for the gift of lamivudine sample.

Electronic Supplementary Information (ESI) available: Crystallographic Information Files (CIFs) under CCDC reference numbers 788023, 788024, 787748, 976187 and 976188; and PDF file loading Tables S1 (crystal data for **2**-**5**), S2 (main torsion angles and planarity descriptors for **1**-**3**), S3 (hydrogen bond table for **2** and **3**)**,** S4 (main bond angles and lengths for **4** and **5**), S5 (main torsion angles for **4** and **5**), and S6 (hydrogen bond table for **4** and **5**); Figures S1 (complete geometry for stacking interactions in **1**-**3**), S2, S3 (ellipsoid plots for **4** and **5**), S4 to S10 (NMR experiments for **4** and **5**), S11, S12 (electrochemical experiments for **4** and **5**), S13 and S14 (infrared spectra for **4** and **5**).

References

1. (a) H. Niinomi, T. Yamazaki, S. Harada, T. Ujihara, H. Miura, H. Kimura, T. Kuribayashi, M. Uwaha and K. Tsukamoto, *Cryst. Growth .Des.*, 2013, **13**, 5188–5192; (b) L. Min-Jeong, C. Nan-Hee, W. In-Chun, L. J. Jay, J. Myung-Yung and J. C. Guang, *Cryst. Growth Des.,* 2013, **13**, 2067–2074; (c) A. Nangia, *Acc. Chem. Res.,* 2008, **41**, 595–604; (d) S. L. Morissette, S. Soukasene, D. Levinson, M. J. Cima and O. Almarsson, *Proc. Natl. Acad. Sci. U. S. A.,* 2003, **100**, 2180–2184. (e) R. Thaimattam, D. S. Reddy, F. Xue, T. C. W. Mak, A. Nangia and G. R. Desiraju, *J. Chem. Soc., Perkin Trans*., 1998, **2**, 1783-1789.

2. (a) G. R. Desiraju, *J. Am. Chem. Soc.,* 2013, **135**, 9952–9967; (b) D. S. Reddy, Y. E. Ovchinnikov, O. V. Shishkin, Y. T. Struchkov and G. R. Desiraju, *J. Am. Chem. Soc.*, 1996, **118**, 4085–4089; (c) G. R. Desiraju, *J. Mol. Struct.,* 1996, **374**, 191–198.

3. (a) T. S. Thakur and G. R. Desiraju, *Cryst. Growth Des.,* 2008, **8**, 4031–4044; (b) J. A. R. P. Sarma, and G. R. Desiraju, *Cryst. Growth Des.,* 2002, **2**, 93–100.

4. F. T. Martins, N. Paparidis, A. C. Doriguetto and J. Ellena, *Cryst. Growth Des.,* 2009, **9**, 5283−5292.

5. (a) C. C. da Silva, M. L. Cirqueira and F. T. Martins, *CrystEngComm,* 2013, **15**, 6311-6317; (b) C. C. da Silva, R. R. Coelho, M. L. Cirqueira, A. C. C. de Melo, I. M. Landre, J. Ellena and F. T. Martins, *CrystEngComm,* 2012, **14**, 4562-4566.

6. (a) L. Rajput, P. Sanphui and G. R. Desiraju, *Cryst. Growth Des.,* 2013, **13**, 3681–3690. (b) P. Sanphui, S. Tothadi, S. Ganguly and G. R. Desiraju, *Mol. Pharmaceutics,* 2013, **10**, 4687–4697; (c) S. R. Perumalla, L. Shi and C. C. Sun, *CrystEngComm,* 2012, **14**, 2389-2390.

7. P. M. Bhatt, Y. Azim, T. S. Thakur and G. R. Desiraju, *Cryst. Growth Des*., 2009, **9**, 951−957.

8. F. T. Martins, R. Bonfilio, M. B. de Araújo and J. Ellena, *J. Pharm. Sci.,* 2012, **101**, 2143-2154.

9. (a) J. Ellena, M. D. Bocelli, S. B. Honorato, A. P. Ayala, A. C. Doriguetto and F. T. Martins, *Cryst. Growth Des.,* 2012, **12**, 5138−5147; (b) F. T. Martins, A. C. Doriguetto and J. Ellena, *Cryst. Growth Des.,* 2010, **10**, 676−684.

10. M. C. Etter, *Acc. Chem. Res.*, 1990, **23**, 120−126.

11. R. K. Harris, R. R. Yeung, R. B. Lamont, R. W. Lancaster, S. M. Lynn and S. E. Staniforth, *J. Chem. Soc. Perkin Trans. 2*, 1997, 2653-2659; (b) J. V. Silverton, F. R. Quinn, R. D. Haugwitz and L. J. Todaro, *Acta Crystallogr., Sect. C,* 1988, **44**, 321-324.

12. J. Ellena, N. Paparidis and F. T. Martins, *CrystEngComm,* 2012, **14**, 2373−2376.

13. (a) H. Chen, J. A. Parkinson, S. Parsons, R. A. Coxall, R. O. Gould and P. J. Sadler, *J. Am. Chem. Soc.,* 2002, **124**, 3064-3082; (b) S. Korn and W. S. Sheldrick, *J. Chem. Soc., Dalton Trans.,* 1997, 2191-2199.

14. M. A. Esteruelas, J. García-Raboso and M. Oliván, *Inorg. Chem.,* 2012, **51**, 9522–9528.

15. A. A. Batista, M. O. Santiago, C. L. Donicci, I. S. Moreira, P. C. Healy, S. J. Berners-Price and S. L. Queiroz, *Polyhedron,* 2001, **20**, 2123-2128.

16. *COLLECT*, Data Collection Software; Nonius: Delft, The Netherlands, 1998.

17. Z. Otwinowski and W. Minor, In *Methods in Enzymology: Macromolecular Crystallography*; C. W. Carter Jr. and R. M. Sweet (Eds.), Academic Press: New York, 1997; Part a, Vol. 276, pp 307-326.

18. G. M. Sheldrick, *Acta Crystallogr., Sect. A,* 2008, **64**, 112−122.

19. C. F. Macrae, I. J. Bruno, J. A. Chisholm, P. R. Edgington, P. Mccabe, E. Pidcock, L. R. Monge, R. Taylor, J. van de Streek and P. A. Wood, *J. Appl. Crystallogr.,* 2008, **41**, 466-470.

20. L. J. Farrugia, *J. Appl. Crystallogr.,* 1997**, 30**, 565.

21. M. Shalaeva, J. Kenseth, F. Lombardo, and A. Bastinz, *J. Pharm. Sci.*, 2008, **97**, 2581-2606.

22. A. Checa, V. G. Soto, S. H. Cassou and J. Saurina, *Anal. Chim. Acta,* 2005, **554**, 177-183.

Figure captions

Scheme 1. Chemical of structures of multicomponent crystal forms and ruthenium coordination complexes studied here.

Figure 1. (a) Asymmetric unit of zalcitabine hydrochloride (**2**) at room temperature. Non-hydrogen atoms are represented as 50% probability ellipsoids, while hydrogens are shown as arbitrary radius spheres. (b) Asymmetric units and (c) crystal structure fragments of lamivudine hydrochloride (**1**)[12] and **2** can be related by pseudo mirror plane (black line).

Figure 2. Supramolecular structure of zalcitabine hydrochloride. One-dimensional chain viewed onto the (a) (100) and (b) (010) planes. Three cross-linked one-dimensional chains viewed onto the (c) (100) and (d) (010) planes. Black circles and box detach hydrogen bonds between the 5'-hydroxyl and 2-carbonyl moieties in panel c. Side one-dimensional chains cross-linked to the center chain as displayed in panels a and b were colored blue and red in both panels c and d. (e) Completing the 3D structure by stacking cytosine rings parallel to the [100] direction. (f) Chloride channels formed parallel to the [100] direction with cytosine stacking distance depicted. Equivalent positions: i = - 1 - x; 0.5 + y; 1 - z; ii = - x; 0.5 + y; - z.

Figure 3. Asymmetric unit of the two-drugs hydrochloride salt of zalcitabine and lamivudine (centre drawing with 50% probability ellipsoids and arbitrary radius spheres for non-hydrogen and hydrogen atoms, respectively) and conformations adopted by the APIs (side ball-and-stick depictions).

Figure 4. Supramolecular structure of the zalcitabine-lamivudine hydrochloride salt **3**. (a) One-dimensional chains made up of only either zalcitabine or lamivudine grow along the *a* axis which are side-to-side packed parallel to the *c* axis, while they are alternately stacked along the *b* axis. (b) View of the alternate face-to-face stacking along the *b* axis of a chain assembled with cytosine stacking distances depicted. (c) Hydrogen bond pattern responsible for assembling the drugs chains (top and bottom illustrations) and for side closing two π-stacked chains related by pseudo centrosymmetry (centre drawing). The antiparallel $(API)^{+}\rightarrow Cl^{-}$ directions along the *a* axis are depicted. (the 5'-CH_2OH atomic fractions of lamivudine with 60% occupancy are not exhibited). (d) API molecules are contacted along the [11-1] direction by mean of π-π base stacking interactions and hydrogen bonds between their 5'-OH moieties (that of lamivudine with s. o. factor of 60% which is shown in this panel). Equivalent positions: i = 1 + x; y; z; ii = - 1 + x; y; z; iii = 1 + x; 1 + y; - 1 + z.

Figure 5. Ruthenium complexes with lamivudine and cytidine (top) can be related by pseudo mirror plane (black line), as well as their nucleoside ligands (shown on the bottom as they are in the structures **4** and **5**). Crystallographically independent cytidine ligand B conformationally differs mainly for cytidine A and lamivudine due to C3'-endo puckering as a consequence of hydrogen bond (dotted white line) between its hydroxyl moiety at this position and the perchlorate counterion (shown).

Figure 6. Packing of ruthenium complexes with nucleoside ligands showing the pseudo mirror plane (black line). PPh_3 moieties were omitted for clarity. Chains containing the cytidine A units are assembled though hydrogen bonds to water molecules disordered over two position sowing 50% occupancy factor each, while that containing cytidine B units show just one-site 50% occupancy water

molecules. The geometry of the main hydrogen bonds stabilizing the crystal structures of **4** and **5** are shown in Table S6.

Table of Contents

Quasi-Enantiomeric Single-Nucleoside and Quasi-Racemic Two-Nucleosides Hydrochloride Salts and Ruthenium Complexes of Cytidine and 2',3'-Dideoxycytidine Analogs Unveiling the Negligible Structure-Driving Role of the 2',3'-Moieties

Felipe Terra Martins, Rodrigo de Souza Corrêa, Alzir Azevedo Batista, Javier Ellena

Synopsis: The role of differences at the 2',3'-positions of the five-membered ring in the determination of molecular conformation and crystal packing of *quasi*-enantiomeric cytidine-based nucleosides from 1) the hydrochloride salt of zalcitabine (2',3'-dideoxycytidine) isostructural to antecedent lamivudine hydrochloride, 2) on the hydrochloride salt having both nucleosides into a single hybrid crystal form, and on the first examples of transition metal coordination complexes with 3) lamivudinate and 4) cytidinate as ligands.

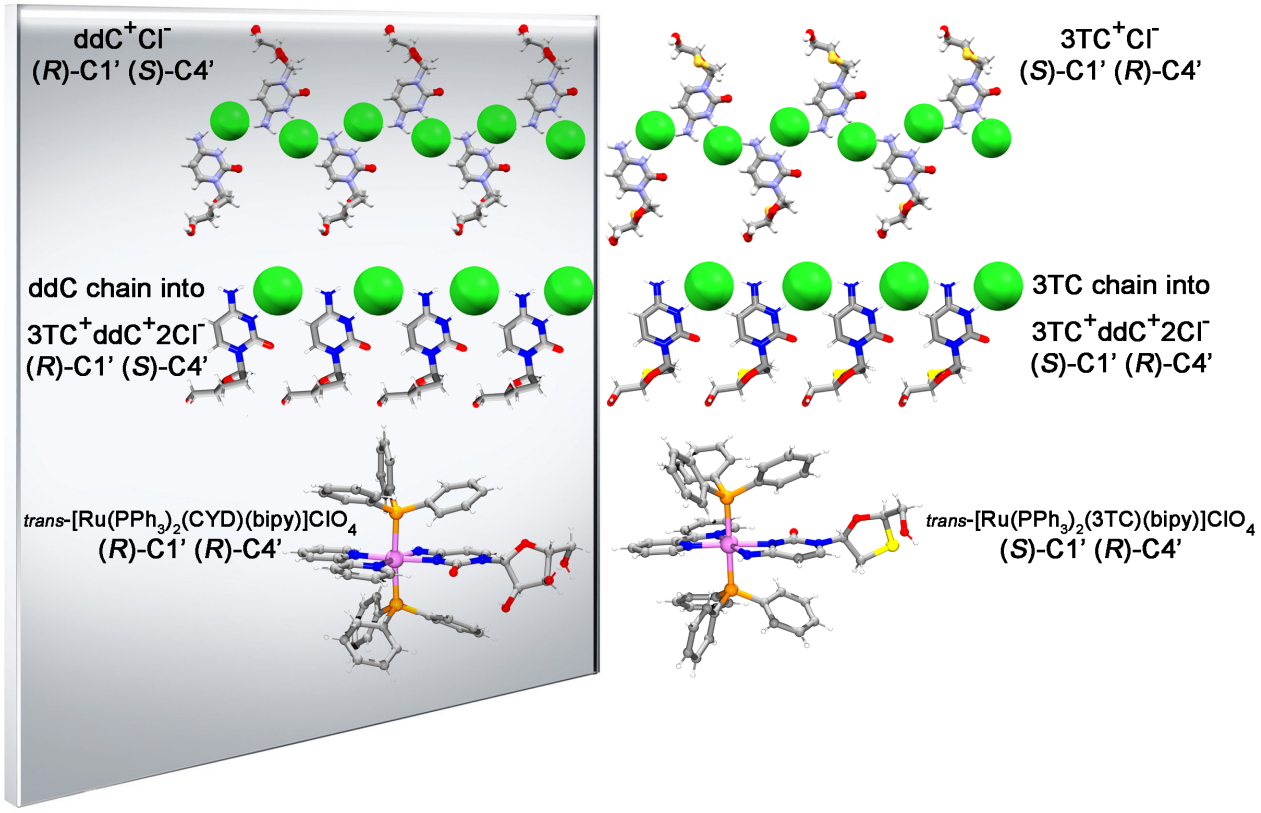

Scheme 1

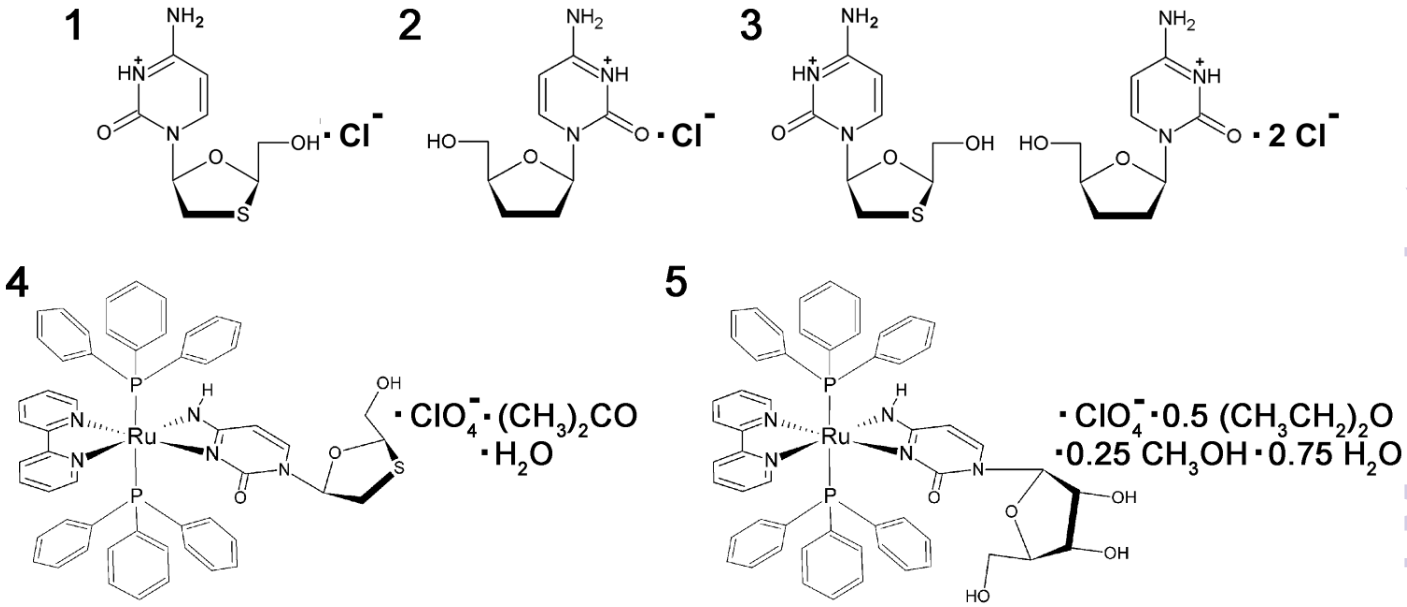

Figure 1

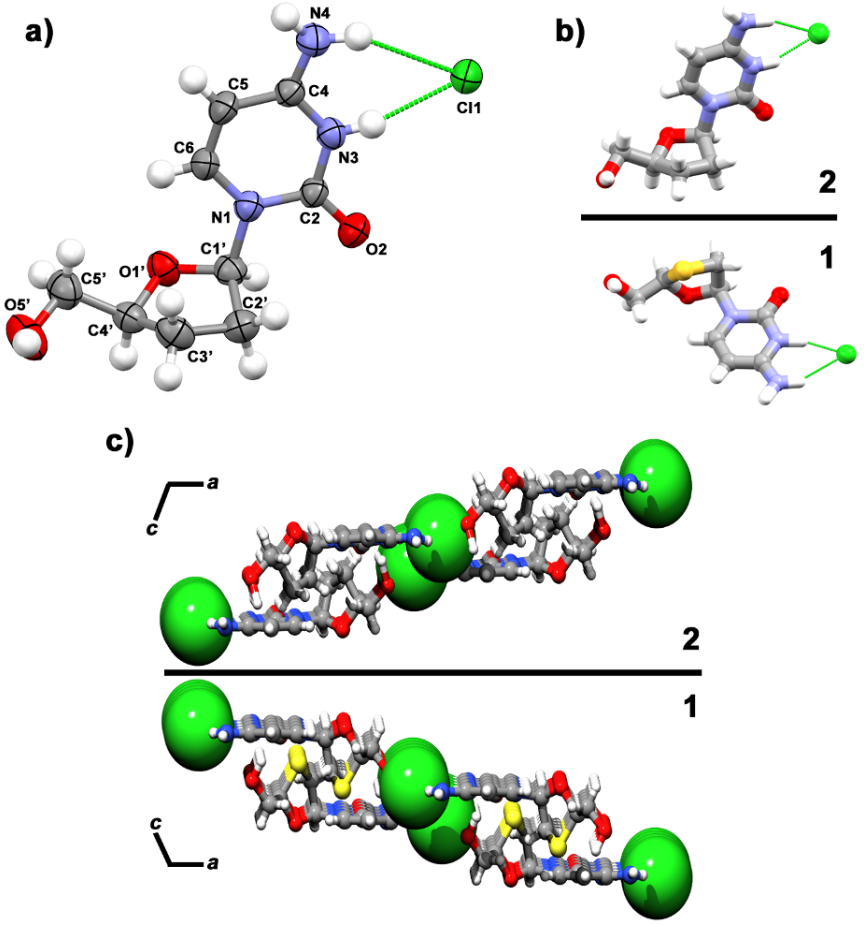

Figure 2

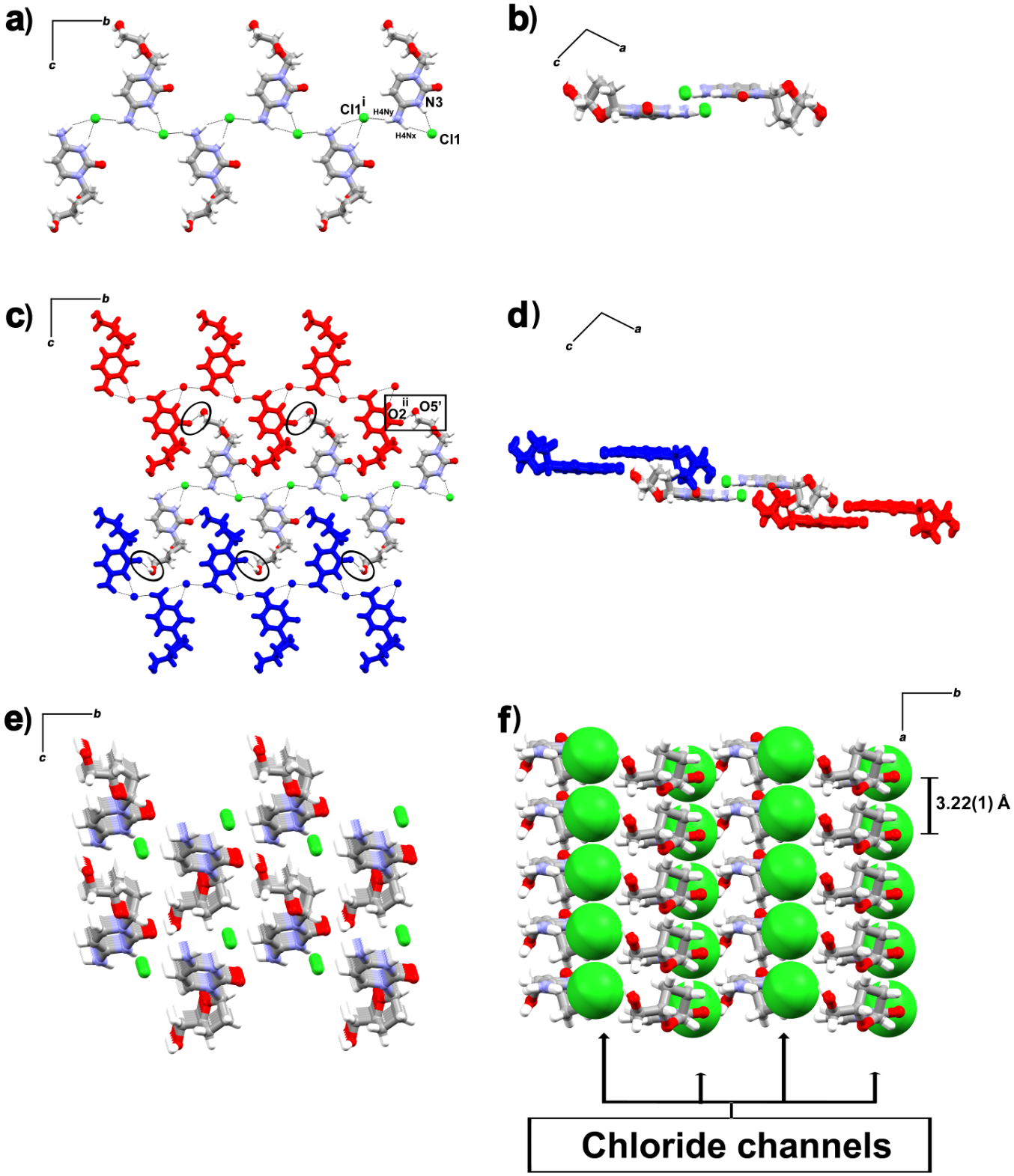

Figure 3

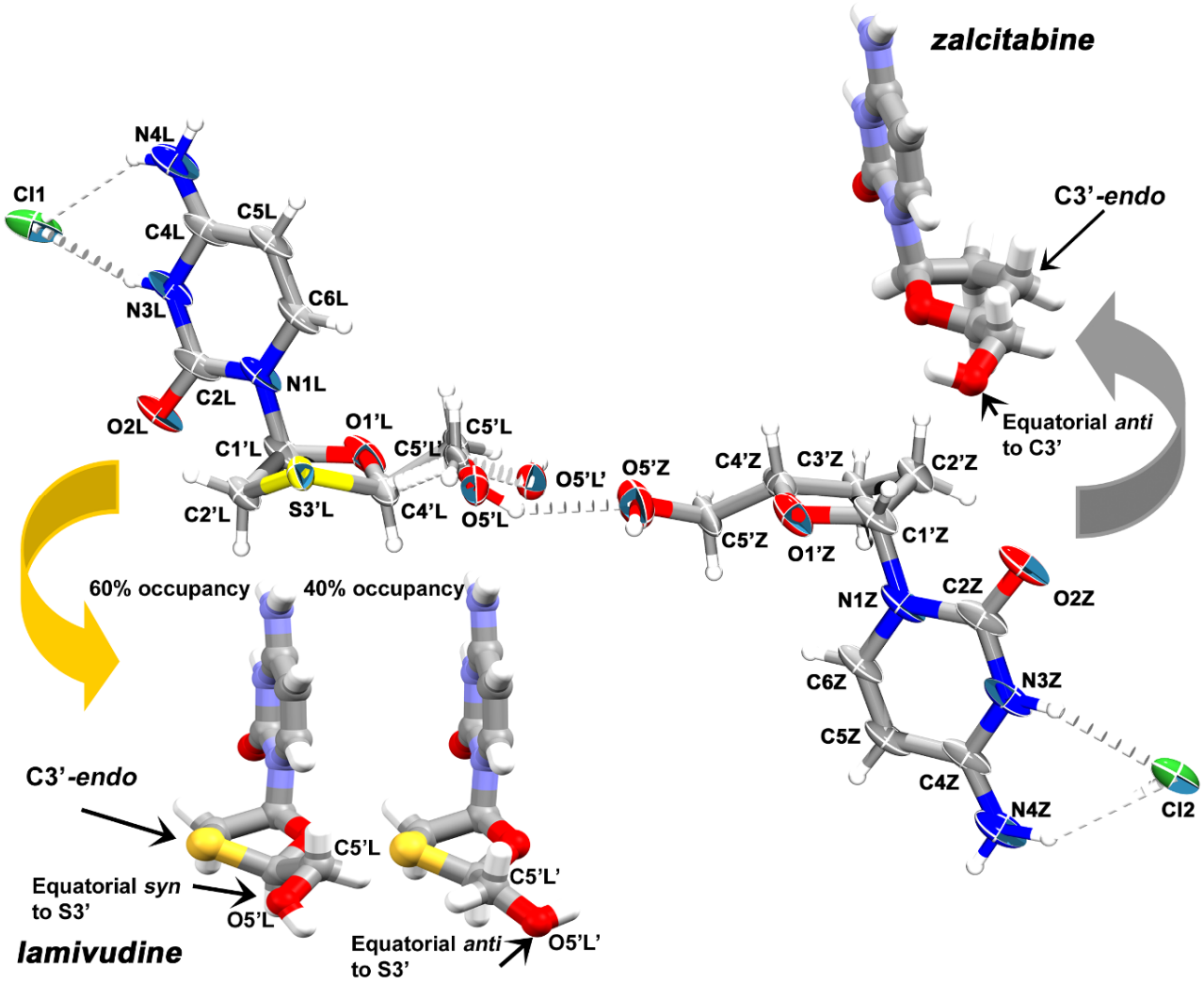

Figure 4

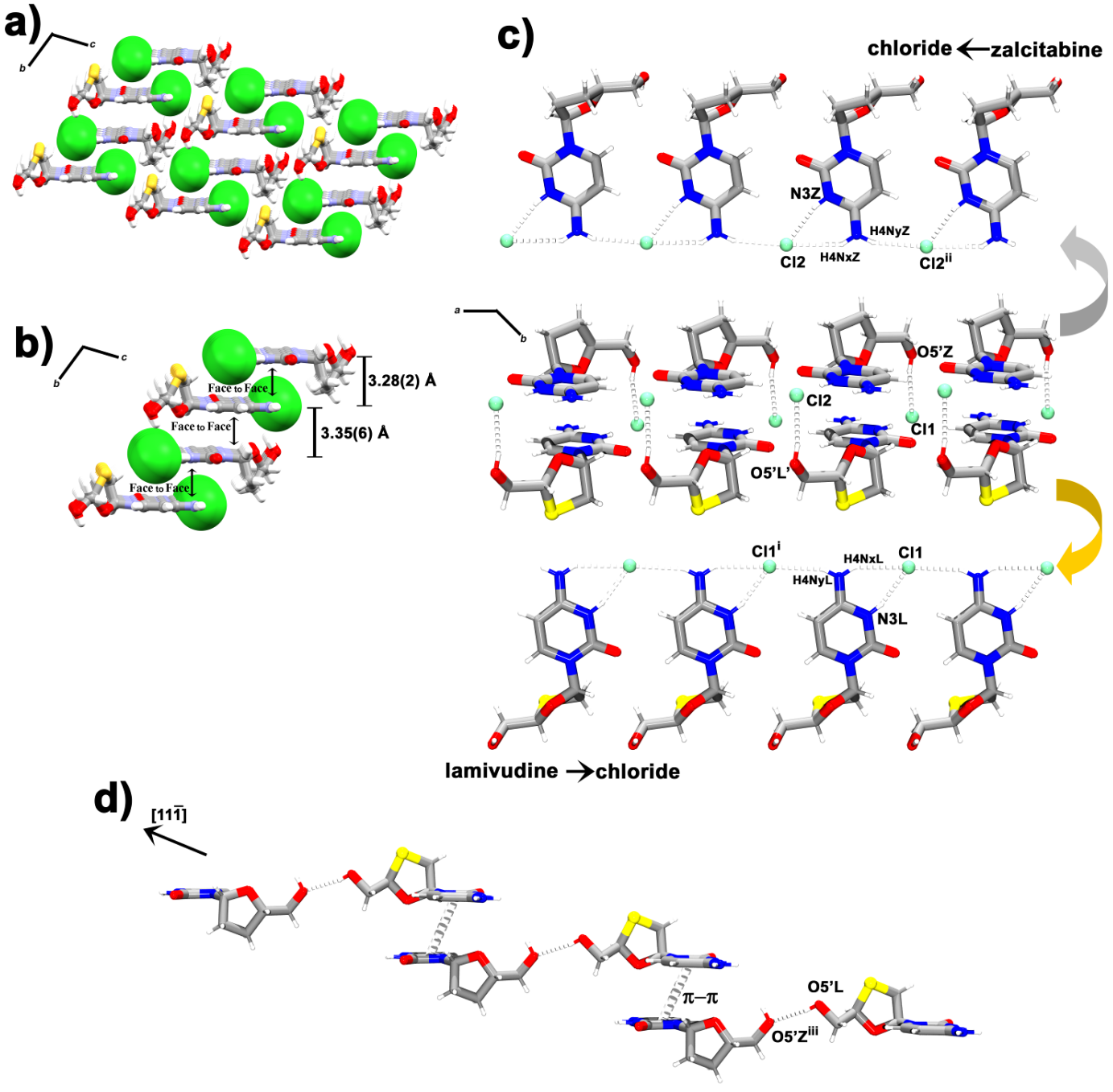

Figure 5

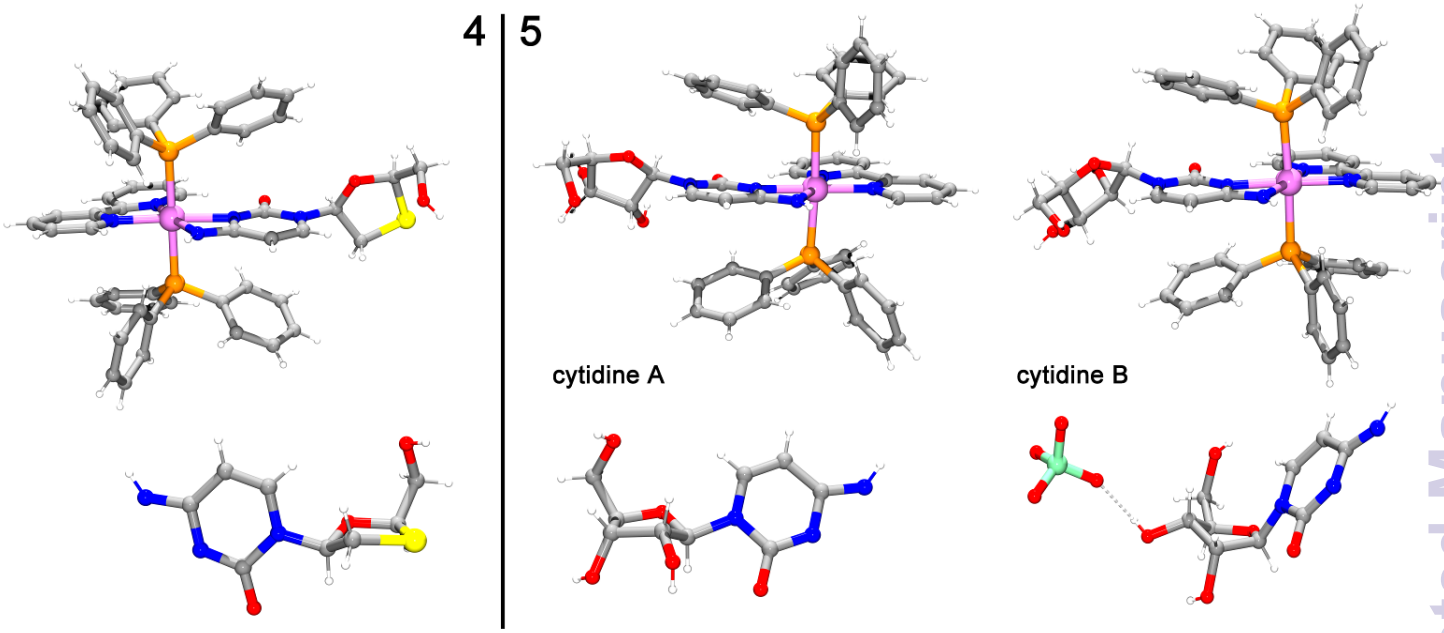

Figure 6